POSITION CONTROL FOR LMCTS WITH NONLINEAR FRICTION AND DETENT FORCE USING DR-FNN CONTROLLER

Jin Woo Lee*, Jin Ho Suh, Young Jin Lee***, Hyun Do Nam****, and Kwon Soon Lee†,[1]**

*,** *Department of Electrical Engineering, National Research Laboratory (NRL), Dong-A University, 840, Hadan-dong, Saha-gu, Busan, 604-714, Korea*
*** *Deptartement of Electrical Instrument and Control, Korea Aviation Polytechnic College, 438 Egeum-dong, Sachon City, Kyungnam, 664-180, Korea*
**** *Department of Electrical Engineering, Dankook University, 8 Hannam-dong, Yongsan-gu, Seoul, 140-714, Korea*
† *Division of Electrical, Electronic and Computer Engineering, National Research Laboratory (NRL), Dong-A University, 840, Hadan-dong, Saha-gu, Busan, 604-714, Korea*

Abstract: This paper presents a position control strategy of the linear motor-based container transfer system (LMCTS) using the soft-computing method. LMCTS is the automatic container transporter in the port. The system has problems to control as weight changes of the mover, the nonlinear friction force, and the detent force, etc. To adapt these problems, we proposed a control system structure that was consisted of two dynamically-constructed recurrent fuzzy neural networks (DR-FNNs). These perform as a controller and a plant emulator with the same structure. And the proposed control system had better performances for the position accuracy and the amount of input consumption than the conventional PID controller and general FNNs with the fixed structure.

Keywords: Linear Motor-based Container Transfer System, position control, detent force, friction, DR-FNN

1. INTRODUCTION

Recently, many technologies have been developed for the yard automation technology. The automated guided vehicle (AGV) had been proposed and has been applied in some ports. However, the AGV had several problems that included the difficulty of control, complexity, low speed, heavy weight, low position accuracy, etc. LMCTS has been developed to solve these problems by simplifying the mechanic system. It is based on the concept of linear motor and rail structure. The main benefits of LMCTS include the high force density and no need for sub-systems. Most importantly, the high precision and accuracy associated with the simplicity in mechanical structure (Franke, 2001). The system can be considered as the huge permanent magnet linear synchronous motor (PMLSM) that is consists of stator modules on the rail and shuttle car. Because of the large variant of mover's weight by the loading and unloading containers, the difference of each characteristic of stator modules, and a stator module's default etc. LMCTS is able to consider as that the system is changed its model suddenly and variously. Then, we will introduce the control strategy that is a multi-step prediction control for LMCTS using two DR-FNNs.

The proposed control system is used the network that is based on fuzzy neural network. It is composed of the structure of neural network that have the fuzzy inference ability and the recurrent loops. In addition, it has ability to adjust the structure of network (Lin *et*

[1] Research supported by the National Research Laboratory Program of the Korea Ministry of Science & Technology (MOST).

al., 2002; Wai and Lin, 2001). Layers in the network are consisted of the adjustable number of nodes which act a role such as the membership function or rule base. We use two units of DR-FNN and each network has two output nodes in the system. One is a predicted system output, another is a predicted reference signal, and others are control input signals from each other network. Then the system has an ability to adapt for the external disturbance, detent force, force ripple, and sudden changes of itself by unifying network weights of controller and emulator.

This paper is organized as follows: Section 2 shows the overview of LMCTS. In Section 3, the proposed control algorithm is described. The computer simulation is conducted in Section 4, followed by the conclusions.

2. MODELING OF LMCTS

2.1 System Dynamics

The system consists of a substructure, shuttle cars, and a control system. The motor style is permanent magnet synchronous linear motor as shown in figure 1. Because of the permanent magnets are installed under the plate of shuttle car, no power cables and other devices are required onto the shuttle car. The considerable shuttle car's dynamic equation is as follow (Lin *et al*., 2002; Wai and Lin, 2001):

$$\ddot{x}=\frac{1}{M}(F_x - f_{friction} - f_{\det} - f_{ripple} - f_{dis} - f_{wind}) \quad (1)$$

where, the various parameters given by (1) are defined by

F_x	thrust force;
M	mass of shuttle car and container;
x	shuttle car position;
$f_{friction}$	friction force;
$f_{\det}$	detent force;
f_{ripple}	force ripple;
f_{dis}	external disturbances;
f_{wind}	wind force.

The major components of force and the relationship between the thrust force, friction, detent force, vertical force, and weight are shown in figure 1. Here, the system input is the bidirectional force on the same stator module that is composed of the longitudinal force F_x and vertical (or lift) force F_z, respectively. Especially, F_z is able to increase or to reduce the shuttle car's mass for the vertical axis only. By these effects, the friction force is changed simultaneously. Therefore it can heighten the acceleration and deceleration performance. The mass of shuttle car is able to modify step function type by loading and unloading container as (2).

$$M_{\min} \le M(t) \le M_{\max} \quad (2)$$

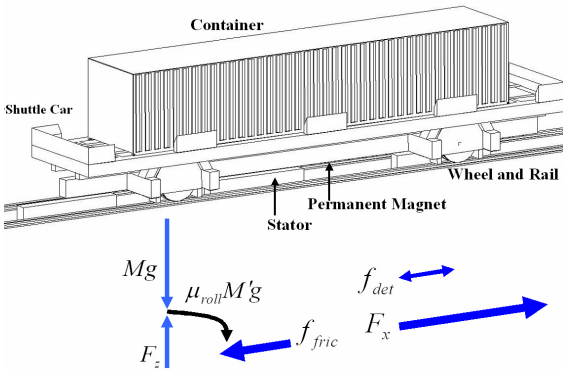

Fig. 1. Configuration and components of LMCTS

where, $M_{\min}$ is only the weight of shuttle car (8 ton) and $M_{\max}$ is the weight of the loaded shuttle car with heaviest container (60 ton). Because the ripple, wind force, and disturbance term are few the amount than the friction and detent force that are the main problem for the position control, these were included to f_e in this paper. Then the considered shuttle car's dynamic equation is described as follow:

$$F_x = M(t)\ddot{x} + f(\dot{x}, \hat{M}) + f_{\det} + f_e \quad (3)$$

where, $\hat{M}$ is considered the changed mass by the levitation force and it influences in the friction force. The thrust force for the longitudinal axis and lift force for the vertical axis are decided by the design according to a mechanical design of a linear motor as shown by figure 2, and then these are described as follows (Yoshida *et al*., 2001):

$$F_x = k_{F0}(\delta) I_1 \sin(\frac{\pi}{\tau}x) \quad (4)$$

$$F_z = -k_{zS}(\delta) I_1^{\,2} - k_{zMS}(\delta) I_1 \sin(\frac{\pi}{\tau}x) \quad (5)$$

where,

k_{F0}, k_{zS}, k_{zMS}	coefficients of thrust force and lift forces concerning the structure parameters of motor;
I_1	effective armature current;
τ	pole pitch;
δ	air-gap length.

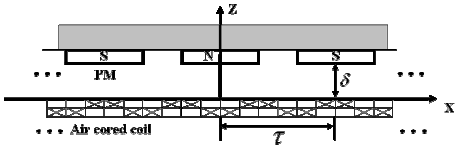

Fig. 2. Part of permanent magnetic synchronous motor below shuttle car frame

Figure 3 is presented the relationship between the thrust and levitation force. The area (a) and (c) are the proposed area to reduce the effect of friction by (Yoshida *et al*., 2001). The area of deceleration is (a) and it is used the positive levitation force. Area (c) is the acceleration area using levitation force with the reduction of friction force. However, we propose the

deceleration area as (b). This area can be used inhalation force with the increase of friction force. Then the quick stop characteristics are respected than (a).

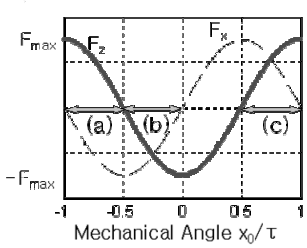

Fig. 3. Areas for acceleration and deceleration, and relationship between longitudinal and vertical and force

To consider the friction model, we used the following type equation in (Lin *et al*., 2002; Wai and Lin, 2001; Wits *et al*., 1994) and it is

$$f_{fric} = [f_c + (f_s - f_c)e^{-(\dot{x}/\dot{x}_s)^2} + f_v\dot{x}]\ sign(\dot{x}). \quad (6)$$

where,

f_c Coulomb friction;
f_s static friction;
f_v viscous friction;
$\dot{x}_s$ lubricant parameter.

However it is need to modify the equation that is included the effect of the mass of shuttle car mass for vertical axis by the container loading/unloading and the use of levitation force. To consider the change by the force, $\hat{M}$ is can be described as (7). By its variation, the changed friction force can be described by (8).

$$\hat{M}(t, F_z) = M(t) - u_{scale}(F_z / g) \quad (7)$$

$$f_{fric} = [\vec{f}_c(\hat{M}) + \{\vec{f}_s(\hat{M}) - \vec{f}_c(\hat{M})\}\ e^{-(\dot{x}/\dot{x}_s)^2} + \vec{f}_v(\hat{M})\dot{x}]\mathrm{sgn}(\dot{x}) \quad (8)$$

where, $\dot{x}_s$ is the experimental coefficient of the reduction velocity from static friction to Coulomb friction in the stribeck effect. Figure 4 shows the friction model that was considered the range of mass variation is 10～60 ton and velocity is -10～10 m/s. In the figure, the area of Ⓐ and Ⓑ is presented the dead zone for the system input. That is, if F_x and other longitudinal forces does not get over the boundary surface, these have no influence with the system (Kim and Lewis, 2000). The included dead zone friction is described as (9).

$$f_{fric}(\dot{x}, \hat{M}) = \begin{cases} f^+_{fric},\ (F_x - f_e) \geq f^+_{fric} \geq 0 \\ (F_x - f_e),\ f^-_{fric} < (F_x - f_e) < f^+_{fric} \\ f^-_{fric},\ (F_x - f_e) \leq f^-_{fric} < 0 \end{cases} \quad (9)$$

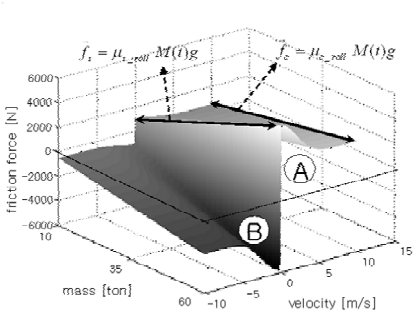

Fig. 4. Friction model of LMCTS with stribeck effect

The detent force can be described as the function for distance, because it depends on the motor magnet configuration. In this study, because the interval between the setup of stator modules is intermittent, it was considered the harmonic sine wave as (10). Where, $K_1(\delta)$ and $K_2(\delta)$ are the gain that are depended on the air gap, permanent magnet size, etc.

$$f_{\det}(x) = K_1(\delta)(15\sin(2\pi x / P + \pi/4 + K_2(\delta)\sin(6\pi x / P + 0.09\pi) \quad (10)$$

2.2 LMCTS Driver System

Figure 5 shows the block-diagram of whole driver system of LMCTS. It is composed of the sensor, input limiter, current coordinate translator, PWM invertor, etc. LMCTS driver is based on the general PMLSM form as follows (Lin *et al*., 2002; Wai and Lin, 2001):

$$v_q = R_s i_q + p\lambda_q + \omega_e\lambda_d \ , \quad v_d = R_s i_d + p\lambda_d - \omega_e\lambda_q \quad (11)$$

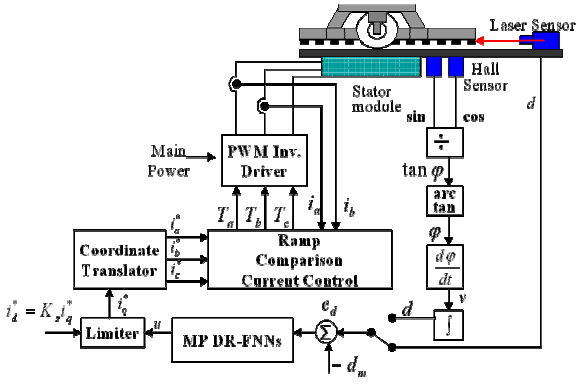

Fig. 5. Block diagram of LMCTS driver system

Flux linkages for each axis, angular velocities, and electric linear velocity are represented by (12) and (13), respectively.

$$\lambda_q = L_q i_q \quad \lambda_d = L_d i_d + \lambda_{PM} \quad (12)$$

$$\omega_e = n_p\,\omega_r \quad \omega_r = \pi v / \tau \quad v_e = n_p\, v = 2\tau\ f_e \quad (13)$$

Electromagnetic power and Electromagnetic force are represented by (14) and (15), respectively.

$$P_e = F_e v_e = 3n_p\{\lambda_d i_q + (L_d - L_q) i_d i_q\} w_e / 2 \quad (14)$$

$$F_e = 3\pi n_p\{\lambda_d i_q + (L_d - L_q) i_d i_q\} w_e / 2\tau \quad (15)$$

where,

v_d , v_q	d-q axis voltages;
i_d , i_q	d-q axis currents;
R_s	phase winding resistance;
L_d , L_q	d-q axis inductances;
ω_r	angular velocity of the mover;
ω_e	electrical angular velocity;
λ_{PM}	permanent magnet flux linkage;
n_p	number of primary poles;
p	differential operator;
v	linear velocity of the mover;
x	distance (mover's position);
τ	pole pitch;
v_e	electric linear velocity;
f_e	electric frequency.

The simplified PMLSM driver and its gain are describe as (16) and (17) respectively. And i_d^*, the levitation force input current, is configured as (18).

$$F_e = K_f i_q^* \quad (16)$$

$$K_F = 3\pi n_p \lambda_{PM} / 2\tau \quad (17)$$

$$i_d^* = K_s \cdot i_q^* \quad (18)$$

3. CONTROL SYSTEM DESIGN

In this paper, the structure of network is composed of having two input and output nodes, respectively. In the proposed control system, two networks are used to the controller and emulator. Figure 6 shows DR-FNN that is used the emulator unit.

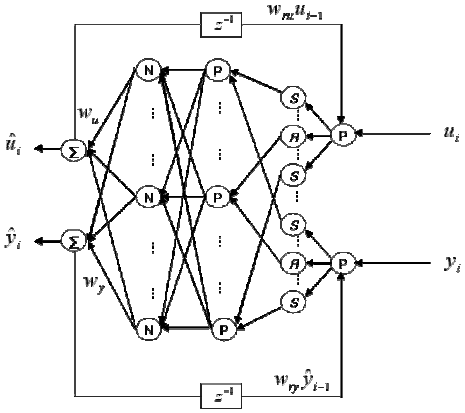

Fig. 6. Structure of DR-FNN unit

One of the output nodes is prediction of the plant output for the one-step ahead, and the other is the predicted control input *u*. And inputs are recurrent delayed values of control input and system output about p-step time index backward. The network can be considered the recurrent style. Because outputs are used inputs these are delayed in next time index.

In figure 6, Layer 1 is the input layer for the linguistic variables. Layer 2 consists of the membership function that has nodes based on the radial basis function. In the case of *j=1* and *u*, for two nodes of edged side in layer 2, the membership function get the shape of sigmoid function, and these are optimized automatically by the back-propagation method. The output of membership function is presented by equation (19) in the second layer (Frayman and Wang, 2002; Widrow and Walach, 1996).

$$\mu_{ij}(x_i) = \exp\left\{-\frac{(x_i - c_{ij})^2}{\sigma_{ij}^2}\right\} \quad (i = 1,2,\ j = 1,2,\cdots,u) \quad (19)$$

where, x_i is the product between the current input and delayed output. x_1 and x_2 are presented by (20).

$$\begin{aligned} x_1(t) &= u(t) \cdot w_{ru} \cdot \hat{u}(t-1) \\ x_2(t) &= y(t) \cdot w_{ru} \cdot \hat{y}(t-1) \end{aligned} \quad (20)$$

Third layer is IF-part for fuzzy rules. For the j-th rule R_j, its output is described by equation (21) in third layer. The normalized output of third layer was calculated in layer 4. It can be expressed by (22).

$$R_k = \exp\left\{-\frac{\sum_{i=1}^{2p}(x_i - c_{ij})^2}{\sum_{i=1}^{2p}\sigma_{ij}^{\ 2}}\right\} \quad (21)$$

$$N_k = R_k / \sum_{l=0}^{N} R_l \quad (22)$$

The fifth (output) layer computes the output of consequence part. Control input and predicted plant output are calculated by (23) and (24) respectively.

$$\hat{y}(t) = \sum_{k=1}^{N} w_{yk} \cdot N_k \quad (23)$$

$$\hat{u}(t) = \sum_{k=1}^{N} w_{uk} \cdot N_k \quad (24)$$

For the prediction and adaptation, DR-FNN is constructed beside plant as an emulator style. The proposed control system is used two DR-FNNs as shown by figure 7.

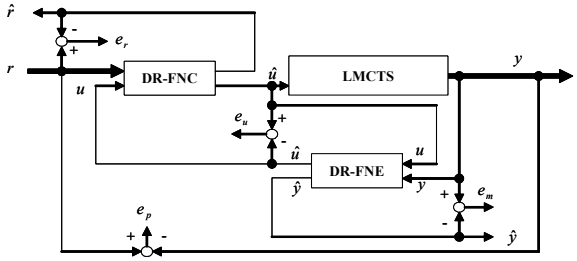

Fig. 7. Control system with DR-FNN controller (DR-FNC) and emulator (DR-FNE)

It performs not only controller but also act of on-line identifier by two outputs from network. The system can obtain predictions of reference input signal $\hat{y}_d$ and the other control input $\hat{u}$. Then, the system has two control inputs protruded from the controller and emulator. In figure 7, the system structure has four errors from networks and plant. Errors and network learning is can be described as follows:

$$e_p = r(t) - y(t),\ E_p = \frac{1}{2}e_p^2$$
$$w'_{l,k}(t+1) = w'_{l,k}(t) + \eta\left\{-\frac{\partial E_p}{\partial w'_{l,k}}\right\} \quad (25)$$

$$e_u = u_c(t-1) - u_e(t-1),\ E_u = \frac{1}{2}e_u^2$$
$$w_{uk}(t+1) = w_{uk}(t) + \eta\left\{-\frac{\partial E_u}{\partial w_{uk}}\right\} \quad (26)$$

$$e_r = r(t+1) - \hat{r}(t+1),\ E_r = \frac{1}{2}e_r^2$$
$$w_{l,k}(t+1) = w_{l,k}(t) + \eta\left\{-\frac{\partial E_p}{\partial w_{l,k}}\right\} \quad (27)$$

$$e_m = y(t) - \hat{y}(t-1),\ E_m = \frac{1}{2}e_m^2$$
$$w'_{l,k}(t+1) = w'_{l,k}(t) + \eta\left\{-\frac{\partial E_m}{\partial w'_{l,k}}\right\} \quad (28)$$

The predicted reference input signal $\hat{y}_d$ and the predicted plant output $\hat{y}$ are trained by e_r. To improve the adaptability in this case, the proposed control scheme is regarded as the predicted the next step system input because two units of DR-FNN are used to a controller and emulator as figure 8. In the part of controller, if DR-FNC were trained enough by the various patterns of reference input signals, network can simulate without the plant virtually using predicted next reference input. Even though network was trained well for some known patterns also, input is the value that can not be guarantee absolutely. And the reference input can be decided by unknown pattern.

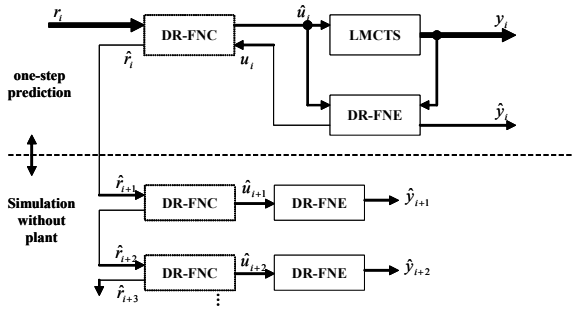

Fig. 8. System structure for multi-step learning

To decide the number of nodes and prediction step, an objective function is needed as the proposed (29). To the system is stable, there is need to minimize Q and to make the value of its gradient to the negative. And it is required preconfigured threshold values $\Delta Q_{\min}$ and $\Delta Q_{\max}$. The structure of the network is regulated by the following rules. In case of (30), the nodes of network are added and the prediction step is reduced. In case of (31), the network keeps its structure. The case of (32) is the number of network nodes is reduced and the prediction step must be increased.

$$Q = \sqrt{\alpha E_p^2 + \beta E_u^2 + \gamma E_r^2 + \delta E_m^2} \quad (29)$$

- Case 1:

  IF $\frac{\partial Q(t)}{\partial t} \geq \Delta Q_{\max}$ (30)

  THEN increase node and reduce prediction step
- Case 2:

  IF $\Delta Q_{\max} \leq \frac{\partial Q(t)}{\partial t} \leq \Delta Q_{\min}$ (31)

  THEN keep the structure of network
- Case 3:

  IF $\frac{\partial Q(t)}{\partial t} < \Delta Q_{\min} \approx 0$ (32)

  THEN decrease node and extend prediction step

4. SIMULATION AND RESULTS

Figure 9 and 10 are the response of open loop system for the test thrust force that type is the half sine wave and its maximum force are 130[kN] and 13[kN] respectively. Figure 10 shows that the effective region is only from 2[sec] to 4[sec] for test input and external force, because of the static rolling friction.

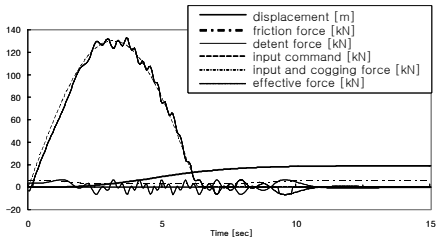

Fig. 9. Open loop system characteristics on the input of half sine wave of maximum 130[kN]

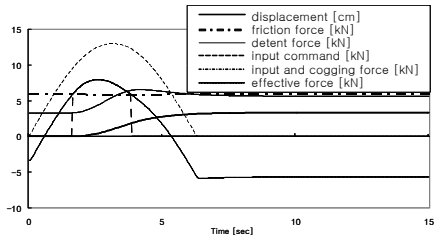

Fig. 10. Minuteness motion characteristics on the input of half sine wave of maximum 13[kN]

In the simulation, the scenario was composed of the following. At first, the empty shuttle car goes until the point of 33m and comes again. Secondly, the container of 40ton is loaded at 50sec. Finally, the loaded shuttle car returns until 55m.

Figure 11 is the result of position error for the PID controller. Gains were tuned by ZN method adding trial and error, FNN controller was used fixed nodes and its structure, the R-FNN that is the recurrent type with the delayed input of network for the position

and the velocity, and the proposed control system with separating to 16 node start from 5 membership functions, respectively. It shows the variation of distance error for the whole range. The maximum position error is less than 1.8cm and the average is about 0.8cm in the stop area. Figure 12 and 13 show the used longitudinal and vertical input, and figure 14 is presented the energy consumption by integrating the scaled RMS value of inputs.

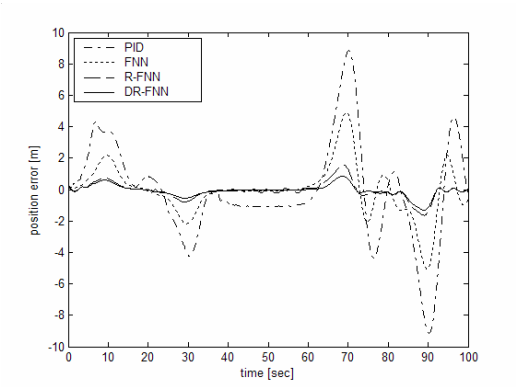

Fig. 11. Position errors

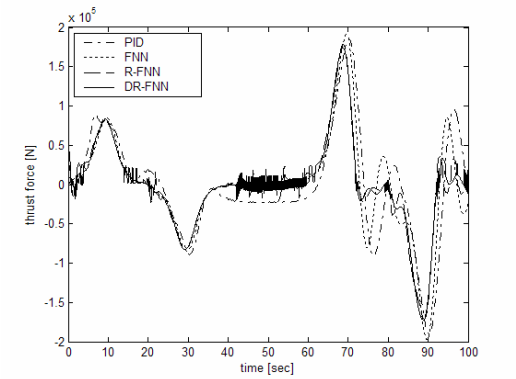

Fig. 12. Thrust forces

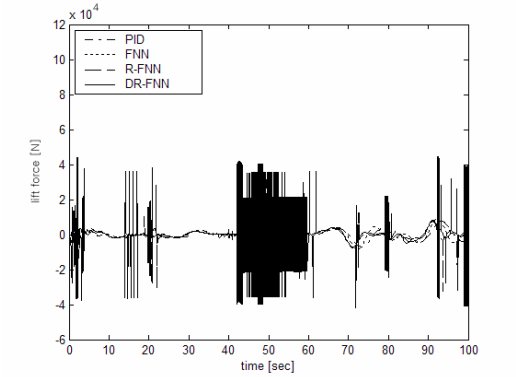

Fig. 13. Vertical forces

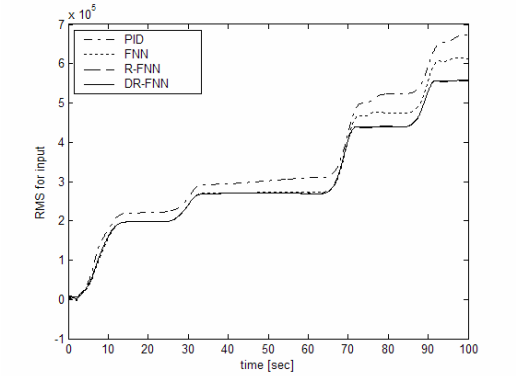

Fig. 14. RMS value of both inputs

5. CONCLUSION

In this study, we modeled LMCTS system by modifying the general PMLSM and adding with the considerable various disturbances. In LMCTS, the system included various kinds of problems to control such as the detent force, force ripple, external disturbances, the variation of mover weight, the periodic lack of thrust force, etc. To improve the positioning accuracy and reduce the energy consumption, we proposed a control system that has multi-step predictable structure using two DR-FNN units. In the case of using DR-FNN, The accuracy was less than 3mm in the stop area. There are improvements of 81%, 68%, and 3% than the PID controller, the supervised FNN, and R-FNN, respectively in position accuracy. By multi-step predictable structure, the amount of control input was reduced about 24.6%, 8.3%, 0.8% than PID controller, FNN, and R-FNN, respectively.

REFERENCES

Brian Armstrong-Helouvry, Pierre Dupont, and Carlos Canudas De Wits 1994, A Survey of Models, Analysis Tools and Compensation Methods for the Control of Machines with Friction," *Automatica*, Vol. 30, No. 7. pp. 1083-1138.

B. Widrow and E. Walach (1996), *Adaptive Inverse Control*, Upper Saddle River, Prentice Hall.

F. J. Lin, R. J. Wai, and C. M. Hong (2002), Hybrid Supervisory Control Using Recurrent Fuzzy Neural Network for Tracking Periodic Inputs, *IEEE Trans. on Neural Networks*, Vol. 12, No. 1, January.

Klaus-Peter Franke (2001), Boosting Efficiency of Split Marine Container Terminals by Innovative Technology, *IEEE Intelligent Transportation Systems Conference Proc*., Oakland, USA, August, pp. 774-779.

K. Yoshida, H. Takami, X. Kong, and A. Sonoda (2001), Mass Reduction and Propulsion Control for a Permanent- Magnet Linear Synchronous Motor Vehicle, *IEEE Trans. on Industry Applications*, Vol. 37, No. 1, pp. 67-72.

Rong-Jong Wai, Faa-Jeng Lin (2001), Adaptive Recurrent- Neural-Network Control for Linear Induction Motor, *IEEE Trans. on Aerospace and Electronic Systems*, Vol. 37, No. 4, pp. 1176-1192.

V. Kecman, L. Vlacic, and R. Salman (1999), Learning in and performance of the new neural network based adaptive backthrough control structure, *Proceedings of the 14-th IFAC Triennial World Congress*, Beijing, PR Chaina, Vol. K, pp. 133-140.

Young Ho Kim and Frank L. Lewis (2000), Reinforcement Adaptive Learning Neural-Net-Based Friction Compensation control for High Speed and Precision, *IEEE Trans. on Control Systems Technology*, Vol. 8, No. 1, pp. 118-126.